Carcinogenesis vol.32 no.5 pp.686–694, 2011
doi:10.1093/carcin/bgr025
Advance Access publication February 10, 2011

Capsaicin promotes a more aggressive gene expression phenotype and invasiveness in null-TRPV1 urothelial cancer cells

Sara Caprodossi[1,2], Consuelo Amantini[1], Massimo Nabissi[1], Maria Beatrice Morelli[1,2], Valerio Farfariello[1,2], Matteo Santoni[1], Angela Gismondi[2] and Giorgio Santoni[1,*]

[1]School of Pharmacy, Section of Experimental Medicine, University of Camerino, Via Madonna delle carceri, 9, 62032 Camerino, Italy and [2]Department of Molecular Medicine, Sapienza University of Rome, 00161 Rome, Italy

[*]To whom correspondence should be addressed. Tel: +39 0737 403312; Fax: +39 0737 403325;
Email: giorgio.santoni@unicam.it

Capsaicin (CPS) has been found to exhibit either tumor promoting or suppressing effects, many of which are mediated by the specific transient receptor potential vanilloid type-1 (TRPV1). Herein, we provide evidence that CPS treatment induced a more aggressive gene phenotype and invasiveness in 5637 cells-lacking TRPV1 receptor. CPS treatment of 5637 cells induced upregulation of pro-angiogenetic (angiopoietin 1, angiopoietin 2 and vascular endothelial growth factor), pro-invasive and pro-metastatic genes (MMP1, MMP9, TIMP1, TIMP3, granzyme A (GZMA), NM23A and S100A) with a downregulation of apoptotic genes (Fas/CD95 and tumor necrosis factor receptor superfamily member 1A). CPS increased the invasiveness of 5637 cells by triggering IGF (insulin-like growth factor)-1 release, GZMA and MMP9 activation, α-tubulin disassembly and cytoskeleton degradation. Finally, in order to evaluate the relationship between the lack of TRPV1 expression and increased CPS-induced invasiveness, we transfected 5637 cells with the TRPV1 complementary DNA (cDNA) sequence. We found that TRPV1-expressing cells show CPS-mediated calcium level increase, growth inhibition and apoptosis. Moreover, CPS-induced migration and MMP9 activation were reverted, suggesting an inhibitory role played by TRPV1 in urothelial cancer cell invasion and metastasis.

Introduction

Capsaicin (CPS, $C_{18}H_{27}NO_3$), the main component in chilli peppers (1), has been shown to inhibit *in vivo* and *in vitro* cancer growth and progression and to induce apoptosis of different cancer cells (2–7); however, at present, its role in cancer is controversial with some reports indicating that CPS also shows carcinogenic effects (8–12). The CPS-induced antitumor effects are mainly mediated by interaction with the transient receptor potential vanilloid type-1 (TRPV1) channel (13–16); however, TRPV1-independent effects have been also reported (7).

TRPV1 is a non-selective cation channel belonging to the TRP family of ion channels (17). In the urinary bladder, TRPV1 is expressed both in the afferent sensory neurons and on the basal and apical urothelial cells (18). Recent evidence suggests that changes in TRPV1 expression appear to be associated with specific early local, or later invasive, stages of urothelial cancers (UCs) with a progressive loss of TRPV1 expression in invasive UCs with respect to non-invasive UCs (16,18). We have recently demonstrated that CPS, a specific-TRPV1 agonist, induced a TRPV1-dependent G_0/G_1 cell cycle arrest and Fas-mediated apoptosis of RT4 UC cells (16). Thus, as the pro-apoptotic role of TRPV1, its higher expression in low-grade UC cells confers susceptibility to CPS-induced apoptosis; in contrast, its reduction/loss in high-grade UCs is associated with resistance to CPS-induced death. Accordingly, we have reported a negative prognostic role of TRPV1 downregulation in the survival of UC patients, demonstrating that reduction of TRPV1 messenger RNA (mRNA) expression represents an independent risk factor for bad disease outcome (19).

Aim of this study was to evaluate the molecular mechanisms responsible for the CPS-induced acquisition of a more aggressive phenotype and the inhibitory role of TRPV1 in CPS-mediated increased invasiveness of 5637 UC cells.

Abbreviations: Ab, antibody; ANGPT, Angiopoietin; cDNA; complementary DNA, CPS; capsaicin, ECM; extracellular matrix, FITC; fluorescein isothiocyanate, GZMA; granzyme A, GZMB; granzyme B, HEPES; *N*-2-hydroxyethylpiperazine-*N*′-2-ethanesulfonic acid, IGF; insulin-like growth factor, MMP; metalloproteinase, MTT; 3-(4,5-dimethylthiazol-2-yl)-2,5-diphenyltetrazolium bromide, mRNA; messenger RNA, pAB; p-aminobenzamide, PAI-1; plasminogen activator inhibitor-1, PBS; phosphate-buffered saline, PCR; polymerase chain reaction, PLAU; plasminogen activator urokinase, PLAUR; plasminogen activator urokinase receptor, RAG; rabbit anti-goat, RT; reverse transcription, TNFRSF1A; tumor necrosis factor receptor superfamily member 1A, TRPV1; transient receptor potential vanilloid type-1, UC; urothelial cancer.

Materials and methods

UC cell lines

Human well differentiated, grade I papillary RT4 and moderately differentiated, grade II/III 5637 UC cell lines, from American Type Culture Collection (Rockville, MD), were maintained in RPMI-1640 medium (Flow Laboratories, Irvine, Scotland) supplemented with 10% heat-inactivated fetal calf serum (Euroclone, Devon, UK), 2.5 mM *N*-2-hydroxyethylpiperazine-*N*′-2-ethanesulfonic acid′ (HEPES), 2mM L-glutamine, 100 IU/ml of penicillin, 100 μg/ml of streptomycin at 37°C, 5% CO_2 and 95% humidity.

Cell transfection

The plasmid encoding human TRPV1 (TRPV1-pCMV) was constructed by introducing in frame TRPV1 cDNA in Bgl II/Hind III pCMV-Fusion Stable Reporter (Genlantis, San Diego, CA)-cloning sites. In total, 5637 UC cells were plated at the density of 1.5×10^5/ml in six-well plates and incubated 12 h at 37°C in a final volume of 1 ml. Twelve micrograms of pCMV or TRPV1-pCMV were added to the wells, following METAFECTENE PRO transfection protocol (Biontex Laboratories, San Diego, CA). Cells were harvested up to day 3 post-transfection.

RNA isolation and reverse transcription

Total RNA was extracted from cell lines using the RNeasy Mini kit (Qiagen, Valencia, CA). In brief, cultured cells were first collected by centrifugation for 5 min at 5000 g, washed in phosphate-buffered saline (PBS) and then processed for total RNA extraction according to manufacturer's instructions. All RNA samples were dissolved in RNAse-free water (Sigma–Aldrich, St Louis, MO) and their concentration and purity were evaluated by A_{260}/A_{280} nm measurement. Two micrograms of RNA were subjected to reverse transcription (RT) using iCycler Thermal Cycler (Bio-rad, Hercules, CA) in a total volume of 50 μl using the High-Capacity cDNA Archive Kit (Applied Biosystems, Foster City, CA) according to protocol. Two microliters of the resulting cDNA were used as template for quantitative polymerase chain reaction (PCR).

Quantitative real-time PCR

TRPV1, IGF-1 and IGF-1R relative expression was evaluated in RT4 and 5637 cells and pCMV- and TRPV1-transfected 5637 by quantitative real-time–PCR by using iQ5 Multicolor Real-Time PCR Detection System (Bio-Rad). β-Actin was used as housekeeping gene to normalize mRNA expression. Human TRPV1 was amplified using the AB RQ Mix (AB Analitica, Padova, Italy) by a thermal protocol consisting of heat activation for 2 min at 50°C and mRNA denaturation for 10 min at 95°C followed by 40 cycles of 95°C for 10 s and 60°C for 1 min. TRPV1 primers and probe were purchased as assay on demand (cod. Hs00218912_m1) by Applied Biosystems. IGF-1 and IGF-1R were amplified by iQ™ SYBR® Green Supermix (Bio-Rad) by a thermal protocol of 95°C for 3 min followed by 40 cycles of 95°C for 10 s, 60°C for 20 s and 72°C for 20 s. Primers and probes relative to IGF-1 (forward 5′-agatgcacaccatgtcctcct-3′, reverse 5′-cacacgaactgaagagcatc-3′); IGF-1R (forward 5′-acgtgaagatccgccattctc-3′, reverse 5′-tggttgtcgaggacgtagaagg-3′) and β-actin (forward 5′-ctggaacggtgaaggtgaca-3′; reverse

5′-cggccacattgtgaactttg-3′; probe 5′-cagtcggttggagcgagcatccc-3′) were designed by Primer Express Software (Applied Biosystems) and purchased from Sigma Genosys (Sigma–Aldrich). All samples were assayed in triplicate in the same plate. The relative amount of target mRNA was calculated by the $2^{-\Delta\Delta Ct}$ method (20).

Western Blot analysis

UC cells resuspended in 0.2 ml of lysis buffer (10 mM Tris, pH 7.4, 100 mM NaCl, 1 mM ethylenediaminetetraacetic acid, 1 mM ethyleneglycol-bis(aminoethylether)-tetraacetic acid, 1 mM NaF, 20 mM $Na_4P_2O_7$, 2 mM Na_3VO_4, 1% Triton X-100, 10% glycerol, 0.1% sodium dodecyl sulfate, 0.5% deoxycholate, 1 mM phenylmethylsulfonylfluoride and protease inhibitor cocktail from Sigma–Aldrich) were lysed by using the Mixer Mill MM300 (Qiagen). Samples were separated on a 7.5% sodium dodecyl sulfate–polyacrylamide gel, transferred onto Immobilon-P membrane (Millipore, Bedford, MA) and blotted with a goat anti-TRPV1 antibody (Ab) (Santa Cruz Biotechnology, Santa Cruz, CA) or a mouse anti-α-tubulin Ab (Sigma–Aldrich), followed by the incubation with horseradish peroxidase-conjugated rabbit anti-goat (RAG) or goat anti-mouse (GAM) Ab (Amersham Biosciences, Uppsala, Sweden), respectively. A mouse horseradish peroxidase-conjugated anti-human glyceraldehyde-3-phosphate dehydrogenase monoclonal Ab (Sigma–Aldrich) was used as protein loading control. Immunoreactivity was detected using enhanced chemiluminescence substrate (Amersham Biosciences). Densitometric analysis was performed by a Chemidoc using the Quantity One Software (Bio-Rad).

Immunofluorescence and flow cytometry

Wild-type and transfected UC cells (3×10^5) were analyzed for TRPV1 and granzyme A (GZMA) expression by using the anti-TRPV1 Ab (Santa Cruz Biotechnolgy) followed by a fluorescein isothiocyanate (FITC)-conjugated RAG Ab and an anti-human FITC-conjugated anti-GZMA monoclonal Ab (Abcam, Cambridge, UK). Briefly, cells fixed and permeabilized using CytoFix/CytoPerm Plus (BD Biosciences, San Jose, CA) were incubated 30 min at 4°C with the primary Ab, washed twice with PBS without calcium and magnesium (Euroclone) and then labeled with the FITC-conjugated RAG Ab (only for TRPV1 detection). The percentage of positive cells, determined >10 000 events was analyzed on a FACScan cytofluorimeter (BD Biosciences) and fluorescent intensity was expressed in arbitrary units on a logarithmic scale.

Calcium influx ($[Ca^{2+}]_i$)measurement

Wild-type and transfected cells (4×10^6/ml) were washed in calcium- and magnesium-free PBS supplemented with 4.5 g/l glucose. Cells were then resuspended in calcium- and magnesium-free PBS/glucose medium supplemented with dimethyl sulfoxide-dissolved 7 μM FLUO 3-AM and 1 μg/ml Pluronic F-127 (Molecular Probes, Eugene, OR) and incubated in the dark for 30 min at 37°C, 5% CO_2. After washing, cells were resuspended in calcium- and magnesium- free PBS/glucose medium containing 2 mM Ca^{2+} and stimulated with CPS (100 μM) and capsazepine (10 μM), alone or in combination. FLUO 3-AM fluorescence was measured on the flow cytometer at 525 nm on the green channel; cells were analyzed for 2 min to establish baseline fluorescence levels.

3-(4,5-dimethylthiazol-2-yl)-2,5-diphenyltetrazolium bromide assay

The colorimetric 3-(4,5-dimethylthiazol-2-yl)-2,5-diphenyltetrazolium bromide (MTT) assay was used to evaluate the growth of CPS-treated wild-type and TRPV1-transfected cells. Briefly, 8×10^3 cells were treated for 24 h at 37°C and 95% of humidity in a 96-well plates with different doses of CPS (10–100 μM). Samples were incubated for the last 3 h with 20 μl/well of MTT (5 mg/ml). Then, supernatants were discarded and colored formazan crystals, dissolved with 100 μl/well of dimethyl sulfoxide were read by an ELISA reader (BioTek Instruments, Winooski, VT) at 570 nm wavelength.

Trypan blue exclusion assay

Cell viability was tested by trypan blue dye exclusion test. Briefly, 5637 cells transfected with TRPV1 or the empty vector were seeded in 24-well plates at a density of 1×10^5 cells/ml in the presence of 100 μM CPS for 24 h in humidified incubator of 5% CO_2 at 37°C. After treatment, cells were washed twice in PBS and they were dissociated with ethylenediaminetetraacetic acid–trypsin solution. Trypan blue (0.4%) was added to cell suspension, and living cells were counted using the Burker chamber. Results were calculated as the percentage (± standard deviation) of the CPS-treated living cells respect the cells grown in the absence of CPS.

Annexin V-FITC/propidium iodide-double staining

In total, 2×10^5 5637 cells transfected with TRPV1 or empty vector were treated with CPS (100 μM) for 24 h at 37°C, 5% CO_2, in a 24-well plates and phosphatidylserine (PS) exposure was detected by annexin V staining. Briefly, cells were stained with annexin V-FITC for 10 min at room temperature and washed once with binding buffer (10 mM HEPES/NaOH, pH 7.4, 140 mM NaCl, 2.5 mM $CaCl_2$). Two micrograms of propidium iodide were added to samples before they were analyzed by a biparametric analysis with a FACScan cytofluorimeter (BD Biosciences) using the CellQuest software.

Assessment of DNA fragmentation

Nucleosomal DNA fragmentation induced by CPS was revealed by agarose gel electrophoresis. Briefly, 1.5×10^6 TRPV1- and empty vector-transfected 5637 cells were treated for 24 h with 100 μM CPS and genomic DNA was extracted by the DNeasy Tissue kit (Qiagen) following the manufacturer's instructions. One microgram of recovered DNA was electrophoresed on 1.5% agarose gel, stained with ethidium bromide and acquired by a ChemiDoc (Bio-Rad).

RT profiler PCR array

Total RNA from RT4 and 5637 cells, untreated or treated for 4 and 12 h with CPS (100 μM), was isolated as above described. Two micrograms of RNA extracted from each sample were subjected to RT in a total volume of 20 μl using the ReactionReady™ first strand cDNA (Superarray Bioscience Corporation, Frederick, MD). RT mixtures were incubated for 60 min at 37°C and 5 min at 95°C. Quantitative RT–PCR was performed using an iQ5 Multicolor Real time PCR Detection system (Bio-Rad), the SuperArray's RT^2 real-time SYBR Green PCR Master Mix and the Human CancerFinder™ plates (Superarray Bioscience Corporation). Each PCR amplification consisted of heat activation for 10 min at 95°C followed by 40 cycles of 95°C for 15 s and 60°C for 1 min. Measurement of five housekeeping gene levels on the samples was used to normalize mRNA content and the expression levels of 84 different genes were represented as relative fold respect to the corresponding control according to the protocol (Superarray Bioscience Corporation).

ELISA assay

In total, 5×10^4 5637 cells were resuspended in complete medium, seeded in a six-well chamber and incubated for different times (6, 12, 18 and 24 h) at 37°C with 100 μM CPS. IGF-1 and GZMA levels were determined by ELISA technique (Quantikine R&D Systems, Minneapolis, MN) according to the manufacturer's instructions. Test sensitivity was 0.026 ng/ml.

Matrigel invasion assay

Cell invasion through a three dimensional extracellular matrix (ECM) was assessed in wild-type and transfected 5637 cells by a Matrigel invasion assay using BD Matrigel Invasion Chambers (BD Biocoat, Bedford, MA), according to manufacturers's instructions. Briefly, 5×10^4 5637 cells were resuspended in 500 μl of the medium and seeded in the upper compartment of the Matrigel-coated insert of the chambers, in presence of 100 μM CPS or 10 nM IGF-1. Medium (500 μl) was added to the lower chambers and the plate was incubated for 24 h at 37°C. At the end of 24 h of incubation, the non-invading cells were removed from the upper surface of the membrane by 'scrubbing'. Invasive cells penetrating to the lower surface of the insert were stained for 20 min with Coomassie brilliant blue. Cell quantification was performed by dissolving stained cells in 10% acetic acid (100 μl/well) and transferring the dye/solute mixture to a 96-well plates for colorimetric reading at 560 nm.

Confocal laser scanning microscopy analysis

In total, 2×10^5/ml 5637 cells grown for 24 h at 37°C and 5% CO_2 in poly-L-lysine-coated slides in presence of 100 μM CPS were permeabilized using 2% paraformaldehyde with 0.5% Triton X-100 in PBS and fixed by 4% paraformaldehyde in PBS. After three washes in PBS, cells were incubated with 3% bovine serum albumin and 0.1% Tween-20 in PBS for 1 h at room temperature and then with a goat anti-TRPV1 Ab (Santa Cruz Biothecnology) overnight at 4°C. Samples were washed three times with 0.3% Triton X-100 in PBS, incubated 1 h at 37°C with RAG Alexa Fluor 488 (Santa Cruz Biotechnology), mounted and analyzed with MRC600 confocal laser scanning microscope (Bio-Rad) equipped with a Nikon (Diaphot-TMD) inverted microscope. Serial optical sections were taken at 1 μm intervals through the cells. Images were processed using Jasc Paint Shop Pro (Jasc Software Inc, Eden Prairie, MN).

Measuring matrix metalloproteinase 9 activity

MMP9 activity was quantified in wild-type and transfected 5637 cells by using the Activity Assay System Biotrak™ MMP9 (GE Healthcare, Waukesha, WI) according to the manufacturer's instructions. Both the endogenous levels of total and active MMP9 have been detected. Briefly, 8×10^5 5637 cells suspended in RPMI medium containing 5% fetal calf serum were plated in a six-well plates and CPS solution was added to wells at final concentration of 100 μM in a total volume of 5 ml. After 24 h of incubation at 37°C protein lysates were prepared and 30 μg of total proteins were diluted in the assay buffer supplied by the kit. The activity of MMP9 was detected by a microplate reader (Biotek Instruments) at 405 nm.

Statistical analysis

Data are reported as the mean ± standard deviation of at least three separate experiments. The statistical significance was determined by Student's *t*-test and by Bonferroni posttest (analysis of variance one way).

Results

Loss of a functional TRPV1 expression in 5637 UC cells

TRPV1 has been found to be highly expressed both at mRNA and protein levels in normal human urothelial cells and low-grade UCs with a progressive decline in high-grade UCs (16,18). Thus, we determined the expression of TRPV1 in 5637 cells, both at mRNA and protein levels (Figure 1A and B). By quantitative real-time–PCR, TRPV1 mRNA levels were significantly reduced as compared with RT4 cells; parallel, by immunoblotting no TRPV1 protein expression was found in 5637 cells. No reactivity was observed with normal goat serum used as control (data not shown).

Since TRPV1 is a cation channel showing high Ca^{2+} sensitivity (17), we evaluated Ca^{2+} influx in UC cells treated with CPS (Figure 1C). We found that CPS rapidly increased $[Ca^{2+}]_i$ levels in RT4 cells in a TRPV1-dependent manner, as evaluated by the ability of the TRPV1 inhibitor, capsazepine (21), to completely revert the CPS-

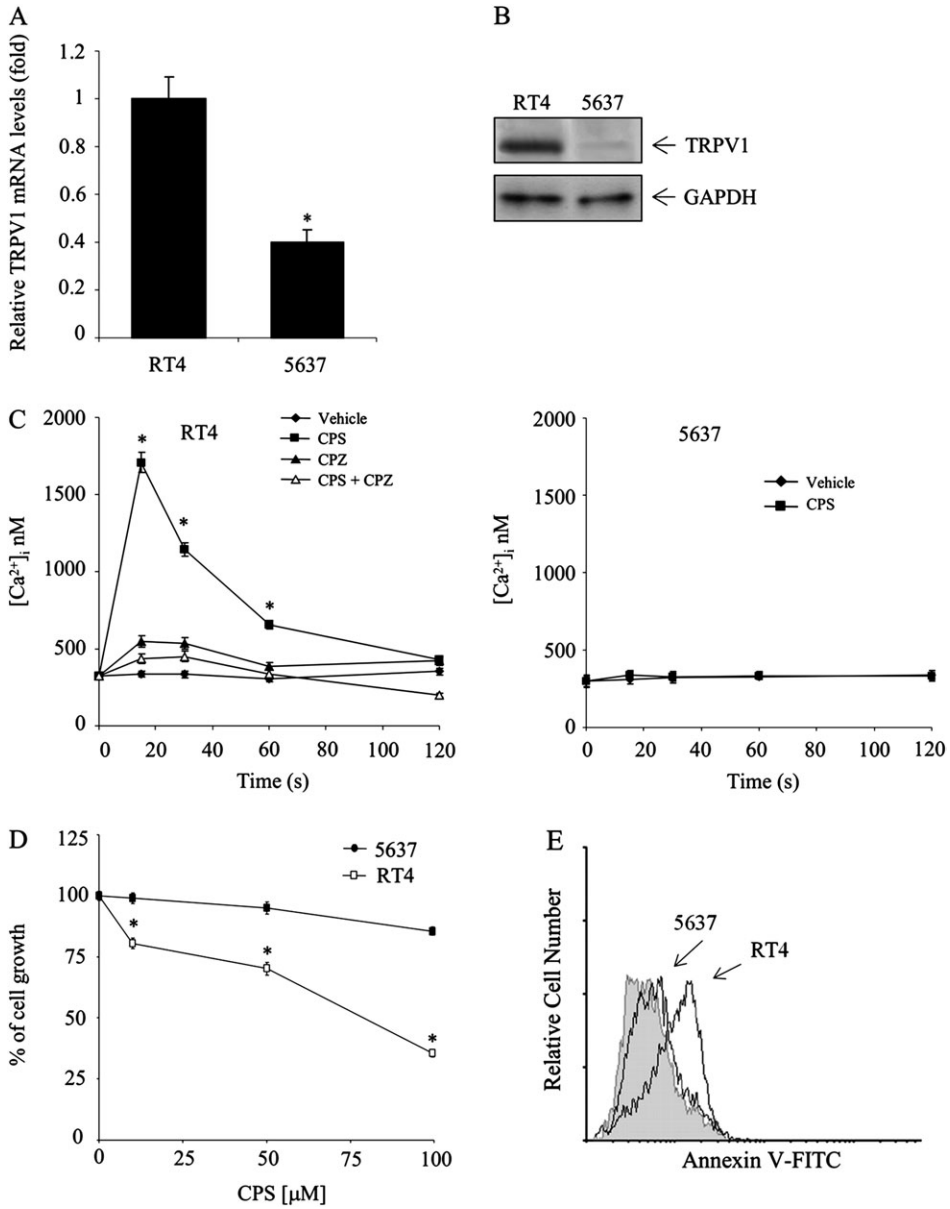

Fig. 1. Functional TRPV1 expression in UC cells. (**A**) TRPV1 mRNA expression in 5637 and RT4 cells was evaluated by quantitative real-time–PCR. TRPV1 mRNA levels (mean ± standard deviation) were expressed as relative fold with respect to RT4 cells used as control. Values were normalized for β-actin expression. $^{*}P \leq 0.01$ as evaluated by Student's t-test. (**B**) Lysates from 5637 and RT4 cells were separated on 7.5% sodium dodecyl sulfate–polyacrylamide gel electrophoresis and probed with a goat anti-human TRPV1 Ab. Anti-human glyceraldehyde-3-phosphate dehydrogenase monoclonal Ab was used as protein loading control. (**C**) CPS-induced rise of $[Ca^{2+}]_i$ influx was evaluated by immunofluorescence and FACS analysis in 5637 and RT4 cells treated for different times with vehicle (dimethyl sulfoxide), CPS (100 μM) or capsazepine (10 μM), alone or in combination. FLUO 3-AM fluorescence was measured on the flow cytometer at 525 nm on the green channel. Statistical analysis was performed by comparing CPS or capsazepine-treated with vehicle-treated cells, and CPS plus capsazepine-treated cells with CPS- or capsazepine-treated cells. $^{*}P \leq 0.01$ as evaluated by Student's *t*-test. (**D**) Cell growth was evaluated by MTT assay in 5637 and RT4 cells, treated for 24 h with different doses of CPS (10, 50 and 100 μM). Statistical analysis was performed comparing the percentage of growth of 5637 cells with that of RT4 cells. $^{*}P \leq 0.01$ as evaluated by Student's *t*-test. (**E**) The percentage of annexin V-positive 5637 and RT4 cells treated for 24 h with 100 μM CPS or vehicle was evaluated by FACS analysis. Gray area represents vehicle-treated UC cells.

mediated effects. In contrast, no $[Ca^{2+}]_i$ increase was found in CPS-treated 5637 cells.

We have previously reported that treatment of RT4 cells with CPS (100 μM) induced cell cycle arrest in G_0/G_1 phase and apoptosis (16). Therefore, we evaluated the ability of CPS to inhibit the growth and induce apoptosis of 5637 UC cells by MTT assay and annexin V staining (Figure 1D and E). We found that 5637 UC cells were completely resistant to CPS-induced apoptotic effects, as compared with RT4 cells. No cell death was observed with vehicle alone both in RT4 and 5637 UC cells.

CPS enhances the invasiveness of 5637 cells

CPS has been found to increase IGF-1 expression in different tissues (22), and a role for IGF-1 and IGF-1R in the establishment of an invasive phenotype by inducing migration of UC cells have been reported (23). Thus, we evaluated the ability of CPS to induce IGF-1 release and promote UC invasion. By RT–PCR, we found that 5637 cells showed higher IGF-1 and IGF-1R mRNA levels compared with RT4 cells (Figure 2A). In addition, CPS induced a 2-fold increase of IGF-1R mRNA levels (data not shown), stimulated Matrigel invasion (Figure 2B) and induced a time-dependent release of IGF-1 in 5637 cells (Figure 2C).

CPS induces an invasive gene expression phenotype in 5637 cells

In an attempt to evaluate the molecular mechanisms underlying CPS-mediated effects, we performed a gene expression profiling in 5637 UC cells at 4 and 12 h after CPS exposure, by using a customized PCR arrays including genes involved in cell cycle control, DNA damage repair, apoptosis, angiogenesis, invasion and metastasis (Table I). Among the 84 defined genes examined, 16 resulted upregulated and 2 downregulated at different times after CPS treatment. In particular, among genes controlling the apoptotic pathways, upregulation of the anti-apoptotic *BCL2* and downregulation of the pro-apoptotic death receptor FAS were observed in CPS-treated cells. In addition, upregulation of genes involved in angiogenesis [angiopoietin (*ANGPT*) 1, *ANGPT2, COL18A1, TEK, TNF* and vascular endothelial growth factor], invasion and metastasis [*MMP1, MMP9, TIMP1, TIMP3, NM23A*, plasminogen activator urokinase (*PLAU*), plasminogen activator urokinase receptor (*PLAUR*), *S100A* and *GZMA*] and downregulation of the protease inhibitor plasminogen activator inhibitor-1 (*PAI-1*) was evidenced.

CPS induces MMP9 and GZMA activity in 5637 cells

Activation of metalloproteinases (MMPs) is considered to be critical for cell migration and invasion of UC cells (24). As MMP1 and MMP9 mRNA were upregulated in CPS-treated 5637 UC cells, we evaluated the ability of CPS to increase and activate MMP9, highly expressed in muscle invasive UCs (24–27), demonstrating that CPS increased the levels of both total (pro-MMP9) and active form of MMP9 (Figure 2D).

As the major role of the PLAU system in cancer invasion and metastasis by inducing MMP9 activation (28) and the increase of PLAU/PLAUR as well as decrease of serine protease inhibitor clade E (PAI-1) mRNAs we found in CPS-treated cells (Table I), we also

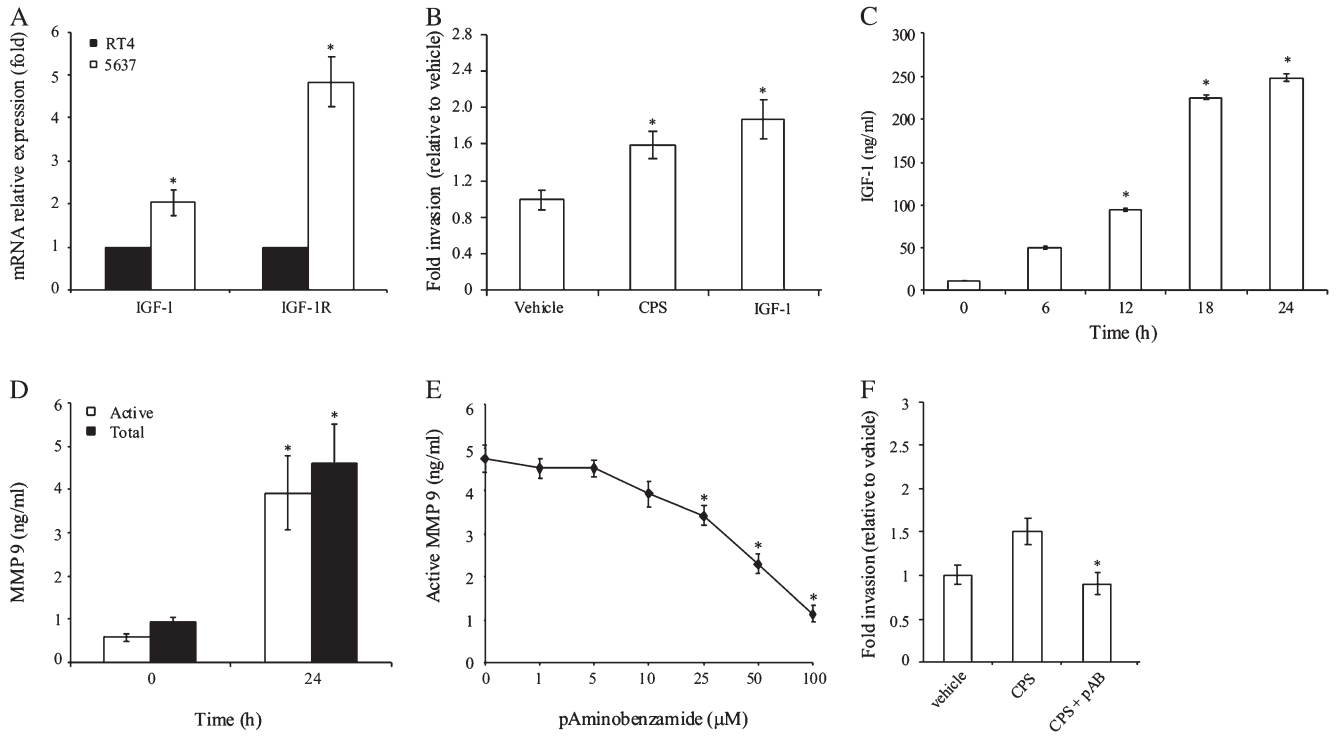

Fig. 2. CPS stimulates invasiveness and induces MMP9 expression and activation in 5637 cells. (**A**) mRNA expression levels of IGF-1 and IGF-1R were evaluated in RT4 and 5637 cells by quantitative real-time–PCR. Values are expressed as relative fold (mean ± standard deviation) with respect to RT4, considering β-actin as housekeeping gene. $^*P \leq 0.01$ as evaluated by Student's *t*-test. (**B**) Cell invasion was evaluated in 5637 cells treated for 24 h with vehicle, 100 μM CPS or 10 nM IGF-1, used as positive control by Matrigel invasion assay. Statistical analysis was performed by comparing CPS or IGF-1 treated with vehicle-treated 5637 cells. $^*P \leq 0.01$, as evaluated by analysis of variance. (**C**) CPS-induced IGF-1 release was evaluated in the supernatant of untreated- or 100 μM CPS-treated 5637 cells at different times (6, 12, 18 and 24 h) by ELISA assay. Statistical analysis was performed by comparing CPS treated (normalized with the relative vehicle treatments) with untreated 5637 cells. $^*P \leq 0.01$ as evaluated by analysis of variance. (**D**) Total and active MMP9 levels were evaluated in 5637 cell lysates at 24 h after 100 μM CPS treatment by MMP9 activity assay. Statistical analysis was performed by comparing CPS with untreated cells, normalized for the relative vehicle. $^*P \leq 0.01$ as evaluated by Student's t-test. (**E**) MMP9 levels were evaluated in 5637 cells treated for 24 h with 100 μM CPS alone or in combination with different doses of pAB by MMP9 activity assay. Statistical analysis was performed by comparing CPS-treated 5637 cells with CPS plus pAB-treated 5637 cells. $^*P \leq 0.01$ as evaluated by Student's *t*-test. (**F**) Cell invasion was evaluated in 5637 cells treated for 24 h with 100 μM CPS in combination with 50 μM pAB, by Matrigel invasion assay. Statistical analysis was performed by comparing CPS plus pAB-treated 5637 cells with CPS-treated 5637 cells. $^*P \leq 0.01$, as evaluated by analysis of variance.

Table I. Changes of gene expression induced by 100 μM CPS in 5637 UC cells

Gene bank ID	Gene description	Fold change	
		4 h	12 h
Apoptosis and cell senescence			
NM_000043	Fas (*FAS*)	−2.6	2.6
NM_000630	B-cell CLL/lymphoma 2(*BCL2*)	6.4	5.1
NM_001065	Tumor necrosis factor receptor superfamily member 1A (*TNFRSF1A*)		3.6
Angiogenesis			
NM_001146	Angiopoietin 1 (*ANGPT1*)	29.2	23.3
NM_001147	Angiopoietin 2 (*ANGPT2*)	4.9	3.0
NM_030582	Collagen type XVIII alpha 1 (*COL18A1*)	2.6	
NM_000459	TEK tyrosine kinase endothelial (*TEK*)	22.5	20.8
NM_003376	Vascular endothelial growth factor (*VEGF*)	5.0	2.5
Invasion and metastasis			
NM_006144	Granzyme A (*GZMA*)	22.2	22.6
NM_002961	S100 calcium-binding protein A4 (*S100A4*)	7.2	4.5
NM_002421	Matrix metalloproteinase 1 (*MMP1*)	2.6	3.8
NM_004994	Matrix metalloproteinase 9 (*MMP9*)	10.4	
NM_000269	Non-metastaic cells 1 protein (NM23A) expressed in (*NME1*)		2.7
NM_002658	Plasminogen activator, urokinase (*PLAU*)		2.5
NM_002659	Plasminogen activator, urokinase receptor (*PLAUR*)		3.0
NM_000602	Serine protease inhibitor, clade E (*PAI-1*)		−2.5
NM_003254	Tissue inhibitor of metalloproteinase 1 (*TIMP1*)		4.7
NM_000362	Tissue inhibitor of metalloproteinase 3 (*TIMP3*)	30.9	24.9

Genes included are ≥2.5-fold upregulated or downregulated with respect to vehicle-treated 5637 cells, used as control. Fold changes >3 have a confidence interval of 99%. Mean of three biological repeats with similar general fold change is presented.

evaluated the ability of p-aminobenzamide (pAB), a plasminogen activator inhibitor (29), to inhibit CPS-mediated effects. Our results showed that pAB completely blocked, in a dose-dependent manner, the CPS-induced MMP9 activation (Figure 2E) and UC invasion (Figure 2F).

As GZMA mRNA level was increased in CPS-treated 5637 cells, we also assessed GZMA expression at protein level by cytofluorimetric and ELISA assays. GZMA protein was expressed in untreated cells, and CPS increased both GZMA expression and release in 5637 cells (Figure 3A and B). In addition, since the ability of GZMA to induce α-tubulin microtubule disassembly in epithelial cells (30,31), we also evaluated the ability of CPS to induce cleavage and microtubule disassembly in 5637 cells. We found that CPS-treated cells showed round morphology and α-tubulin disassembly (Figure 3C) as compared with vehicle-treated cells showing an organized microtubule structure. In addition, two major bands of 51 and 36 kDa, probably corresponding to full length and a cleaved form of α-tubulin, were found in cell lysates of CPS-treated cells (Figure 3D) but not in vehicle-treated cells, suggesting that, similarly to granzyme B (GZMB) (32), GZMA is able to cleave the α-tubulin.

Loss of TRPV1 is responsible of CPS-induced invasive phenotype in 5637 cells

A progressive decrease in TRPV1 expression was found in high-grade invasive UCs (16,18). Therefore, to evaluate the relationship between reduction of TRPV1 expression and increased CPS-induced invasiveness, we transfected TRPV1 cDNA into 5637 cells. As evaluated by RT–PCR and cytofluorimetric analysis increased TRPV1 mRNA and protein expression were found in TRPV1-transfected 5637 cells as compared with pCMV-transfected cells (Figure 4A and B). Transfected TRPV1 was functional since the ability of CPS to increase $[Ca^{2+}]_i$ levels (Figure 4C). Interestingly, as demonstrated by MTT assay, CPS was able to inhibit cell growth in a dose-dependent manner of TRPV1- but not vector-transfected 5637 cells (Figure 4D). Similar results were found by Trypan blue exclusion assay (percentage of growth at 100 μM CPS, TRPV1-5637: 72.1 ± 0.8; pCMV-5637: 98.3 ± 0.2). The mechanism was TRPV1 dependent since the ability of capsazepine to revert CPS-mediated effects (Figure 4E). As described previously (33), CPS at higher doses (500 μM) induced massive cytotoxic effects independently from TRPV1 expression. CPS induced apoptosis as evidenced by the percentage of annexin V-positive apoptotic cells and the characteristic ladder pattern of DNA fragments observed (Figure 5A and B). Finally, transfection of TRPV1 in 5637 cells inhibited the CPS-induced increase of total and active MMP9 levels (Figure 5C) and completely reverted the CPS-mediated Matrigel invasion (Figure 5D).

Overall, the expression of a functional TRPV1 receptor in 5637 cells restored the sensitivity of UC cells to CPS-induced apoptosis and inhibited the CPS-induced acquisition of a more aggressive metastatic phenotype by the 5637 cells.

Discussion

Several studies indicate that tumor progression is associated with changes in the expression of TRPV channels, leading to an uncontrolled expansion and invasion (34,35). Changes involving the TRPV channels may have a promoting role in cancer by increasing the expression of active TRPV receptors in the plasma membrane of cancer cells, thus promoting Ca^{2+}-dependent proliferative pathways. Alternatively, altered expression of TRPV channels may offer a survival advantage, such as resistance of cancer cells to apoptosis (34,35). Therefore, the availability of TRPV receptors at the cell surface of cancer cells becomes critical for its function.

We have previously reported the expression of functional TRPV1 in normal human urothelial cells and low-grade UC cells and the ability of CPS to inhibit the growth of TRPV1-expressing RT4 cells by inducing apoptosis (16). Herein, we found that 5637 cells, lacking of TRPV1, show no changes in $[Ca^{2+}]_i$ levels, also at the higher (300 μM) dose of CPS treatment and are resistant to CPS-mediated apoptosis. Thus, expression of TRPV1 in UC cells determines their life or death under CPS treatment.

By RT profiler PCR assay, we demonstrated the ability of CPS to modulate a number of genes involved in apoptosis, angiogenesis, invasion and metastasis. Among genes controlling the apoptotic cell death, upregulation of anti-apoptotic *BCL-2* and parallel

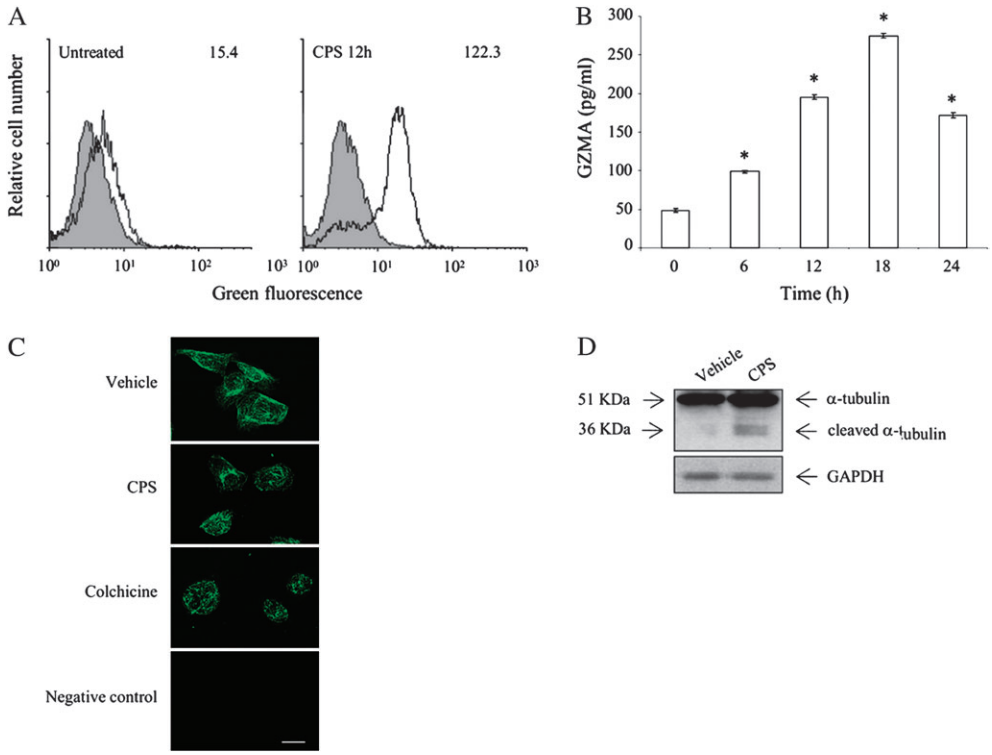

Fig. 3. CPS stimulates GZMA release and induces microtubule disassembly in 5637 cells. (**A**) GZMA expression was evaluated in untreated and 100 μM CPS-treated 5637 cells at 12 h after treatment by using a FITC-conjugated anti-human GZMA mAb and cytofluorimetric analysis. Numbers in the corner represent the mean fluorescence intensity. Gray areas represent the isotype-matched mAb used as negative control. (**B**) GZMA release was evaluated in the supernatant of untreated and 100 μM CPS-treated 5637 cells at different times (6, 12, 18 and 24 h) by ELISA. Statistical analysis was performed by comparing CPS treated with untreated 5637 cells, normalized with the relative vehicle treatments. $^{*}P \leq 0.01$, as evaluated by analysis of variance. (**C**) Microtubule disassembly was evaluated by confocal microscopy in vehicle (dimethyl sulfoxide) or 100 μM CPS-treated 5637 cells. Colchicine (500 μM) treatment was performed as positive control. Rabbit anti-human α-tubulin and FITC-conjugated goat anti-rabbit were used as primary and secondary Ab, respectively. Negative control: secondary Ab alone. Bar = 10 μm. (**D**) Thirty micrograms of total protein lysate from 5637 cells treated for 24 h with 100 μM CPS or vehicle were separated on 8% sodium dodecyl sulfate–polyacrylamide gel electrophoresis and probed with a mouse anti-human α-tubulin Ab, followed by an incubation with an horseradish peroxidase-conjugated goat anti-mouse Ab. Horseradish peroxidase-conjugated anti human glyceraldehyde-3-phosphate dehydrogenase mAb was used as protein loading control.

downregulation of pro-apoptotic *FAS* death receptor were observed in 5637 cells. Conversely, we have reported in RT4 cells, expressing TRPV1, that CPS decreases the levels of the anti-apoptotic *BCL-2* gene, increases FAS mRNA and protein expression, induces a TRPV1-dependent redistribution and clustering of FAS as well as induces apoptosis (16).

In addition, we found that in 5637 cells CPS upregulates the expression of genes involved in cancer invasion and metastasis such as *IGF-1, IGF-1R, MMP1, MMP9, TIMP1, TIMP3, PLAU, PLAUR, GZMA, S100A4* and *NM23A*.

CPS has been demonstrated either to suppress or promote the migration of different cancer cells; in particular, it is able to inhibit B16-F10 melanoma cell migration and invasion by targeting PI3-K/Akt/Rac1 pathway (36) but has also been found to stimulate the migration of HepG2 hepatoma cells induced by hepatocyte growth factor (37). In addition, CPS-mediated denervation/inactivation of TRPV1-expressing sensory neurons also promotes a more aggressive gene expression phenotype and induces mammary tumor metastasis to lung and heart (38,39).

Stimulation of sensory neurons by CPS increases tissue levels of IGF-1 and IGF-1 mRNA in various organs (22). The IGF-1 and IGF-1R have been found to be overexpressed in invasive UC tissues as compared with non-malignant controls (23,40). IGF-1 induces Akt and mitogen-activated protein kinase-dependent phosphorylation of paxillin in 5637 cells, which relocates at dynamic focal adhesions thus promoting motility of bladder cancer cells (23); moreover, IGF-1R has been found to play a critical role in the establishment of invasive phenotype in UCs. In this regard, we found that 5637 cells express high levels of IGF-1 and IGF-1R mRNA as respect to RT4 cells; CPS treatment enhances the IGF-1R mRNA expression, induces IGF-1 release and increases the migration/invasion of 5637 cells.

Metastatic disease is responsible for the majority of cancer-related death and remains the greatest barrier to cancer cure (41) and degradation of the basement membrane and invasion of ECM are considered to be initial steps of the metastatic process (27). These events are mainly dependent on the action of MMPs, endopeptidases, which breakdown ECM proteins. High MMP1 and MMP9 levels in patients with advanced bladder cancers are already described (24–27). Our findings evidenced that CPS increases MMP9 and MMP1 as well as TIMP1 and TIMP3 mRNA levels, enhances total MMP9 level and induces MMP9 activation in 5637 cells. TIMP-1 binds and inhibits MMP9, however, a clear association between increased levels of TIMP1 and TIMP3 expression, progression and recurrence of bladder cancer tumors has been reported (42).

The urokinase plasminogen system is believed to play an important role in cell migration, angiogenesis, cancer cell invasion and metastasis (28), and in transitional cell carcinoma of human bladder higher expression of PLAU and PLAUR mRNAs have been found to characterize a more aggressive phenotype (43). By causing MMP activation, the PLAU/PLAUR pathway induces ECM degradation that results in increased invasion (28).

In this regard, we found that CPS significantly increases PLAU and PLAUR mRNA levels, as well as induces a decrease of the PAI-1 mRNA expression in 5637 cells; moreover, as reported in prostate cancer cells (29), pAB, a potent serine protease inhibitor, completely reverts CPS-induced MMP9 activation and Matrigel invasion, suggesting that inhibition of MMP9 activation by pAB blocks the CPS-mediated UC invasion.

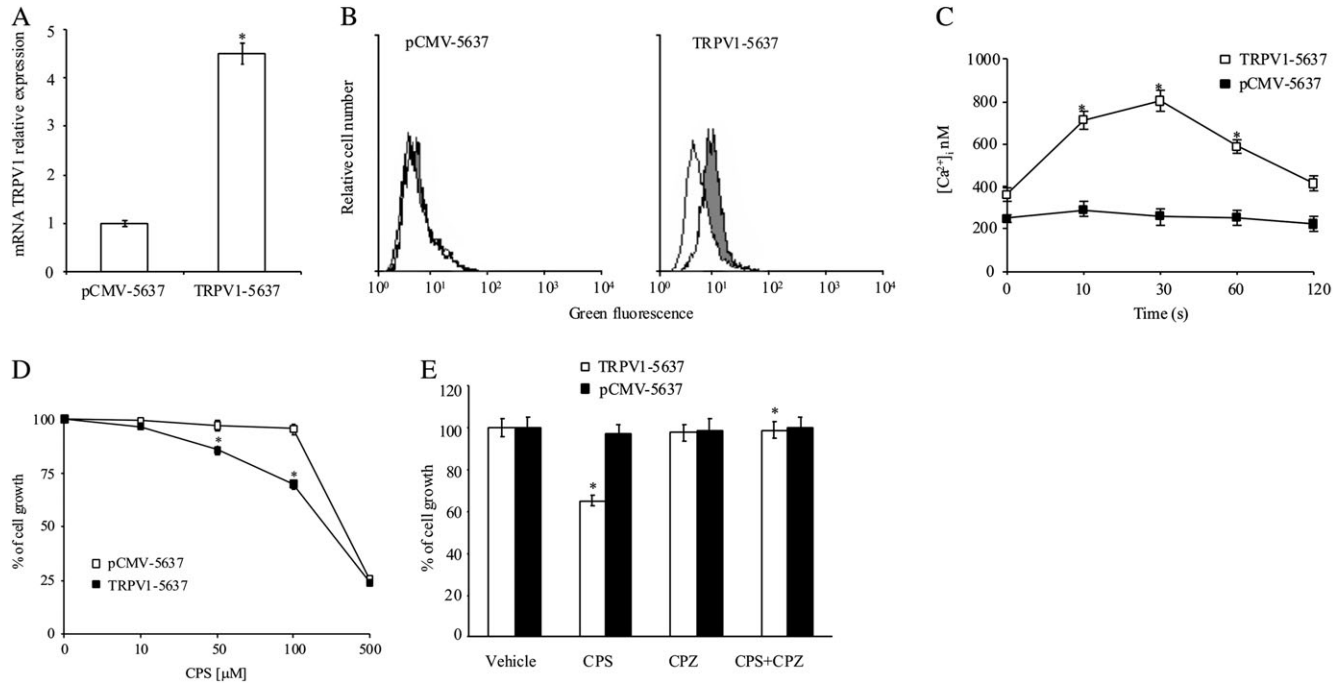

Fig. 4. TRPV1 transfection in 5637 cells stimulates CPS-induced $[Ca^{2+}]_i$ and inhibits cell growth. (**A**) TRPV1 mRNA levels of pCMV- and TRPV1-transfected 5637 cells were evaluated by quantitative real-time–PCR. Values (mean ± standard deviation), normalized for β-actin expression, represent the relative fold with respect to pCMV-transfected 5637 cells. $^*P \leq 0.01$ as evaluated by Student's *t*-test. (**B**) TRPV1 protein expression was evaluated by immunofluorescence and FACS analysis in pCMV-5637 cells (transfected with the empty vector) and TRPV1-transfected 5637 cells (transfected with a TRPV1-containing vector), using a goat anti-human TRPV1 Ab. FITC-conjugated RAG was used as secondary Ab. Gray area of both graphics is referred to the signal produced by the primary Ab; white area indicates the signal of secondary Ab alone used as negative control. (**C**) $[Ca^{2+}]_i$ was evaluated by cytofluorymetric analysis in pCMV- and TRPV1-transfected 5637 cells treated with 100 μM CPS at different times. Values were normalized with vehicle (dimethyl sulfoxide) treatment. Statistical analysis was performed by comparing TRPV1-transfected with pCMV-transfected CPS-treated 5637 cells. $^*P \leq 0.01$. (**D**) Cell growth was evaluated by MTT assay in pCMV- and TRPV1-transfected 5637 cells treated with different doses of CPS (10, 50, 100 and 500 μM). Statistical analysis was performed by comparing CPS-treated cells with vehicle-treated cells. $^*P \leq 0.01$, as evaluated by Student's *t*-test. (**E**) Cell growth was evaluated by MTT assay in TRPV1-transfected 5637 cells treated for 24 h with vehicle, 100 μM CPS, 10 μM capsazepine alone or in combination. Statistical analysis was performed by comparing CPS- or capsazepine- with vehicle-treated cells and CPS plus capsazepine- with CPS-treated cells. $^*P \leq 0.01$; ns, not significative.

GZMA and GZMB are serine proteinases known to be expressed by cytotoxic lymphocytes and involved in apoptosis (32). Like in these cells, GZMA is expressed in alveolar (31) and small intestinal epithelial cells (30), and GZMB is detected in UCs where promotes cancer cell invasion (44). GZMA produced by cytotoxic T lymphocytes mediates apoptosis, whereas in epithelial cells it is not involved in apoptosis but induces disassembly of the microtubule structure, disruption of α-tubulin and detachment of epithelial cells from basement membrane (31). At present, no data on GZMA expression in UCs have been provided so far. By RT–PCR, we firstly provide evidence on the expression of GZMA transcripts in 5637 cells, which are strongly increased (22-fold) by CPS treatment. GZMA protein is constitutively expressed in 5637 cells and CPS treatment increases its expression and induces a time-dependent release. Moreover, we also found that CPS induces rounding of 5637 cells, disassembly of microtubule meshworks and disruption of α-tubulin, as evaluated by the presence of a cleaved form of α-tubulin in cell lysates. Thus, similarly to the recently reported GZMB-mediated promotion of UC cell invasion (32,44), we hypothesized that CPS, by increasing the GZMA expression and function, could contribute to depolymerization of the microtubule network and enhance the invasive capability of 5637 cells.

In addition, overexpression of S100A4 and NM23A mRNA was found in CPS-treated 5637 cells. S100A4 functions as regulator of metastasis in different human tumors and has been implicated in cytoskeleton–membrane interaction, migratory behaviors and malignancy in cancer cells. In accordance with our findings, overexpression of S100A4 was associated with stage progression, invasion and poor survival of bladder cancers (45–47). The NM23 gene is associated with expression of a metastatic phenotype. It has been reported that its expression regulates the biological behavior of tumor cells and confers invasive and metastasizing properties by affecting the state of tubulin polymerization (48). Therefore, the overexpression of S100A4 and NM23 mRNA we found in CPS-treated 5637 cells, further strengthens for a role of CPS in the promotion of a more aggressive phenotype in UC cells.

Changes in the TRPV1 expression occurs during the development of human UCs. We have demonstrated in UCs a progressive decrease in TRPV1 expression as tumor stage increases, with a complete loss in high-grade and stage invasive UCs (16,18). CPS has been found to induce a TRPV1-dependent Fas/CD95-mediated apoptosis in low-grade UCs, whereas high-grade UCs were resistant to CPS-induced cell death (16). Herein, we found that transfection of TRPV1 in TRPV1-lacking 5637 induces a $[Ca^{2+}]_i$ rise in CPS-treated cells, inhibits growth and restores the susceptibility to CPS-induced apoptosis, whereas it does not affect pCMV-transfected UC cells.

Finally, the expression of TRPV1 in transfected 5637 cells completely reverts the CPS-induced MMP9 activation and Matrigel invasion, strongly supporting that TRPV1 expression is negatively associated with UC cells invasive behavior.

Overall, these findings strengthen for a protective role of TRPV1 in UC progression; loss of TRPV1 expression in CPS-treated UC cells results in a more aggressive gene phenotype and increased invasiveness. The knowledge of the molecular mechanisms controlling TRPV1 expression in UCs would be of importance not only for a better understanding of growth and progression of UCs but also for the clinical relevance of TRPV1 agonists in the therapy of superficial urothelial malignancies and to improve the appropriate selection of postoperative follow-up protocols for patients showing a high risk to develop metastatic spreading.

A

	PI+	PI+/AnV+	AnV+	PI -/AnV -
pCMV-5637	2.5 ± 0.3	3.8 ± 0.4	3.2 ± 0.9	90.5 ± 3.1
TRPV1-5637	1.9 ± 0.4	3.1 ± 0.6	30.0 ± 2.3*	66.0 ± 2.2*

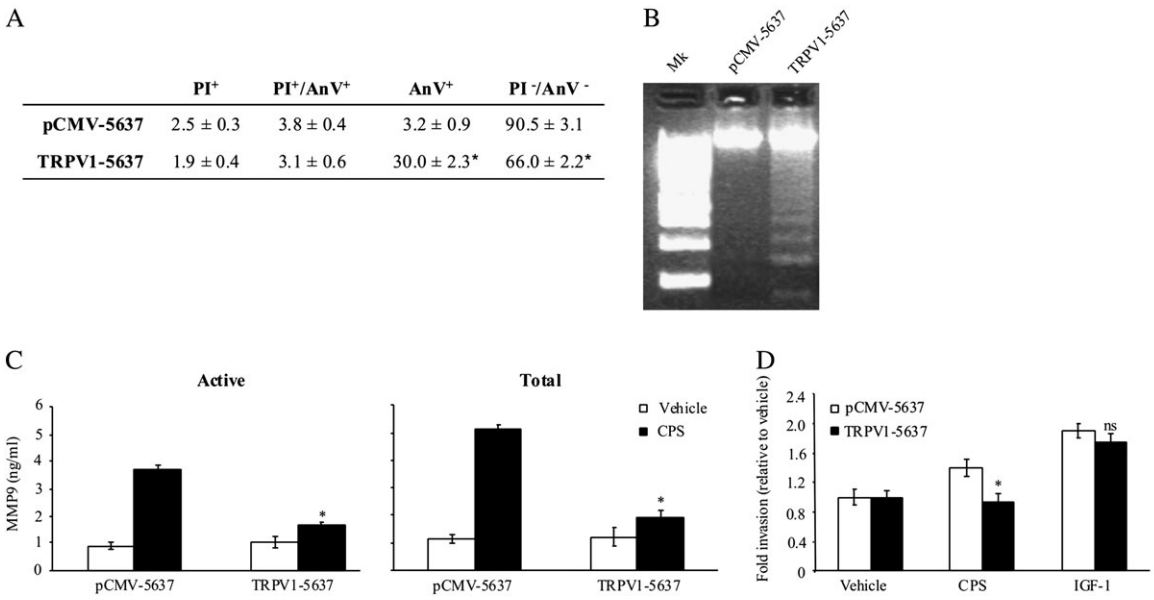

Fig. 5. CPS induces apoptosis, inhibits MMP9 activation and Matrigel invasion in TRPV1-transfected 5637 cells. (**A**) The apoptosis of pCMV- and TRPV1-transfected 5637 cells treated for 24 h with 100 μM CPS was evaluated by biparametric cytofluorimetric analysis using propidium iodide and FITC-conjugated annexin V. Data expressed as percentage of positive cells are the mean (± standard deviation) of three separate experiments. $^{*}P \leq 0.01$, as evaluated by Student's *t*-test. (**B**) DNA fragmentation from pCMV- and TRPV1-transfected 5637 cells treated for 24 h with 100 μM CPS was visualized by 1.5% agarose gel elecrophoresis. Data shown are representative of two separate experiments. Mk: low range DNA marker. (**C**) Total and active MMP9 levels were evaluated by MMP9 activity assay in pCMV- and TRPV1-transfected 5637 cell lysates after 24 h of 100 μM CPS treatment. Statistical analysis was performed by comparing TRPV1- with pCMV-transfected 5637 cells. $^{*}P \leq 0.01$, as evaluated by Student's *t*-test. (**D**) Invasion was evaluated in pCMV- and TRPV1-transfected 5637 cells treated for 24 h with vehicle, 100 μM CPS and 10 nM IGF-1 (as positive control) by Matrigel invasion assay. Statistical analysis was performed by comparing TRPV1- with pCMV-transfected 5637 cells. $^{*}P \leq 0.01$ as evaluated by analysis of variance; ns, not significative.

Funding

Associazione Italiana per la Ricerca sul Cancro Regional Studentship 2008 (6353); University of Camerino.

Conflict of Interest Statement: None declared.

References

1. Szallasi,A. *et al*. (1999) Vanilloid (Capsaicin) receptors and mechanisms. *Pharmacol. Rev.*, **51**, 159–212.
2. Morrè,D.J. *et al*. (1995) Capsaicin inhibits preferentially the NADH oxidase and growth of transformed cells in culture. *Proc. Natl Acad. Sci. USA.*, **92**, 1831–1835.
3. Macho,A. *et al*. (1999) Selective induction of apoptosis by capsaicin in transformed cells: the role of reactive oxygen species and calcium. *Cell Death Differ.*, **6**, 155–165.
4. Hail,N.Jr (2003) Mechanisms of vanilloid-induced apoptosis. *Apoptosis*, **8**, 251–262.
5. Ito,K. *et al*. (2004) Induction of apoptosis in leukemic cells by homovanillic acid derivative, capsaicin, through oxidative stress: implication of phosphorylation of p53 at Ser-15 residue by reactive oxygen species. *Clin. Cancer Res.*, **10**, 2120–2130.
6. Kim,S. *et al*. (2004) Capsaicin-induced apoptosis of H-ras-transformed human breast epithelial cells is Rac-dependent via ROS generation. *Arch. Pharm. Res.*, **27**, 845–849.
7. Mori,A. *et al*. (2006) Capsaicin a component of red peppers, inhibits the growth of androgen-independent, p.53 mutant prostate cancer cells. *Cancer Res.*, **66**, 3222–3229.
8. Toth,B. *et al*. (1992) Carcinogenicity of lifelong administration of capsaicin of hot pepper in mice. *In Vivo*, **6**, 59–63.
9. Agraval,R.C. *et al*. (1986) Tumor-promoting effect of chilli extract in BALB/c mice. *Int. J. Cancer*, **38**, 689–695.
10. Surh,Y.J. *et al*. (1995) Capsaicin, a double-edged sword: toxicity, metabolism, and chemopreventive potential. *Life Sci.*, **56**, 1845–1855.
11. Surh,Y.J. *et al*. (1996) Capsaicin in hot chili pepper: carcinogen, co-carcinogen or anticarcinogen? *Food. Chem. Toxicol.*, **34**, 313–316.
12. Lopez-Carrillo,L. *et al*. (1994) Chili pepper consumption and gastric cancer in Mexico: a case-control study. *Am. J. Epidemiol.*, **139**, 263–271.
13. Contassot,E. *et al*. (2004) Arachidonylethanolamide induced apoptosis of human glioma cells through vanilloid receptor-1. *J. Neuropathol. Exp. Neurol.*, **63**, 956–963.
14. Kim,S.R. *et al*. (2006) Transient receptor potential vanilloid subtype 1 mediates microglial cell death *in vivo* and *in vitro* via Ca2+-mediated mitochondrial damage and cytochrome c release. *J. Immunol.*, **177**, 4322–4329.
15. Amantini,C. *et al*. (2007) Capsaicin-induced apoptosis of glioma cells is mediated by TRPV1 vanilloid receptor and requires p38 MAPK activation. *J. Neurochem.*, **102**, 977–990.
16. Amantini,C. *et al*. (2009) Triggering of Transient Receptor Potential Vanilloid Type 1 (TRPV1) by Capsaicin induces Fas/CD95-mediated apoptosis of urothelial cancer cells in an ATM-dependent manner. *Carcinogenesis*, **30**, 1320–1329.
17. Caterina,M.J. *et al*. (1997) The capsaicin receptor: a heat-activated ion channel in the pain pathway. *Nature*, **389**, 816–824.
18. Lazzeri,M. *et al*. (2005) Transient receptor potential vanilloid type 1 (TRPV1) expression changes from normal urothelial to transitional cell carcinoma of human bladder. *Eur. Urol.*, **48**, 691–698.
19. Kalogris,C. *et al*. (2010) Expression of transient receptor potential vanilloid-1 (TRPV1) in urothelial cancers of human bladder: relation to clinico-pathological and molecular parameters. *Histopathology*, **57**, 744–752.
20. Livak,K.J. *et al*. (2001) Analysis of relative gene expression data using real-time quantitative PCR and the 2(-Delta Delta C(T)) method. *Methods*, **25**, 402–408.
21. Bevan,S. *et al*. (1992) Capsazepine: a competitive antagonist of the sensory neurone excitant capsaicin. *Br. J. Pharmacol.*, **107**, 544–552.
22. Harada,N. *et al*. (2007) Stimulation of sensory neurons by capsaicin increases tissue levels of IGF-I, thereby reducing reperfusion-induced apoptosis in mice. *Neuropharmacol.*, **52**, 1303–1311.
23. Metalli,D. *et al*. (2010) The insulin-like growth factor receptor I promotes motility and invasion of bladder cancer cells through Akt- and mitogen-activated protein kinase-dependent activation of paxillin. *Am. J. Pathol.*, **176**, 2997–3006.

24. Wallard,M.J. *et al*. (2006) Comprehensive profiling and localisation of the matrix metalloproteinases in urothelial carcinoma. *Br. J. Cancer*, **94**, 569–577.
25. Ozdemir,E. *et al*. (1999) Role of matrix metalloproteinase-9 in the basement membrane destruction of superficial urothelial carcinomas. *J. Urol.*, **161**, 1359–1363.
26. Papathoma,A.S. *et al*. (2000) Prognostic significance of matrix metalloproteinases 2 and 9 in bladder cancer. *Anticancer Res.*, **20**, 2009–2013.
27. Kanayama,H. (2001) Matrix metalloproteinases and bladder cancer. *J. Med. Invest.*, **48**, 31–43.
28. Dass,K. *et al*. (2008) Evolving role of uPA/uPAR system in human cancer. *Cancer Treat. Rev.*, **34**, 122–136.
29. Festuccia,C. *et al*. (1998) Plasminogen activator system modulates invasive capacity and proliferation in prostatic tumor cells. *Clin. Exp. Metastasis*, **16**, 513–528.
30. Hirayasu,H. *et al*. (2008) A lymphocyte serine protease granzyme A causes detachment of a small-intestinal cell line (IEC-6). *Biosci. Biotechnol. Biochem.*, **72**, 2294–2302.
31. Yoshikawa,Y. *et al*. (2008) Granzyme A causes detachment of alveolar epithelial A549 cells accompanied by promotion of interleukin-8 release. *Biosci. Biotechnol. Biochem.*, **72**, 2481–2484.
32. Goping,I.S. *et al*. (2006) Identification of {alpha}-tubulin as a granzyme B substrate during CTL-mediated apoptosis. *J. Cell Sci.*, **119**, 858–865.
33. Meddings,J.B. *et al*. (1991) Capsaicin effects on non-neuronal plasma membranes. *Biochem. Biophys. Acta.*, **1070**, 43–50.
34. Bödding,M. (2007) TRP proteins and cancer. *Cell Signal.*, **19**, 617–624.
35. Prevarskaya,N. *et al*. (2007) TRP channels in cancer. *Biochem. Biophys. Acta*, **1772**, 937–946.
36. Shin,D.H. *et al*. (2008) Inhibitory effect of capsaicin on B16-F10 melanoma cell migration via phosphatidylinositol 3-kinase/Akt/Rac1 signal pathway. *Exp. Mol. Med.*, **40**, 486–494.
37. Waning,J. *et al*. (2007) A novel function of capsaicin-sensitive TRPV1 channels: involvement in cell migration. *Cell Calcium*, **42**, 17–25.
38. Erin,N. *et al*. (2004) Capsaicin-mediated denervation of sensory neurons promotes mammary tumor metastasis to lung and heart. *Anticancer Res.*, **24**, 1003–1009.
39. Erin,N. *et al*. (2006) Capsaicin-induced inactivation of sensory neurons promotes a more aggressive gene expression phenotype in breast cancer cells. *Breast Cancer Res. Treat.*, **99**, 351–364.
40. Zhao,H. *et al*. (2003) Plasma levels of insulin-like growth factor-1 and binding protein-3, and their association with bladder cancer risk. *J. Urol.*, **169**, 714–717.
41. Gupta,G.P. *et al*. (2006) Cancer metastasis: building a framework. *Cell*, **127**, 679–695.
42. Durkan,G.C. *et al*. (2003) Alteration in urinary matrix metalloproteinase-9 to tissue inhibitor of metalloproteinase-1 ratio preducts recurrence in nonmuscle-invasive bladder cancer. *Clin. Cancer Res.*, **9**, 2576–2582.
43. Bhuvarahamurthy,V. *et al*. (2004) In situ expression of urokinase-type plasminogen activator in transitional cell carcinoma of the human bladder. *Oncol. Rep.*, **12**, 909–913.
44. D'Eliseo,D. *et al*. (2010) Granzyme B is expressed in urothelial carcinoma and promotes cancer invasion. *Int. J. Cancer*, **127**, 1283–1294.
45. Yao,R. *et al*. (2007) The S100 proteins for screening and prognostic grading of bladder cancer. *Histol. Histopathol.*, **22**, 1025–1032.
46. Agerbaek,M. *et al*. (2006) Focal S100A4 protein expression is an independ predictor of development of metastatic disease in cystectomized bladder cancer patients. *Eur. Urol.*, **50**, 777–785.
47. Matsumoto,K. *et al*. (2007) Expression of S100A2 and S100A4 predicts for disease progression and patient survival in bladder cancer. *Urology*, **70**, 602–607.
48. Lakshmi,M.S. *et al*. (1993) Metastasis associated MTS1 and NM23 genes affect tubulin polymerisation in B16 melanomas: a possible mechanism of their regulation of metastatic behaviour of tumours. *Anticancer Res.*, **13**, 299–303.

Received September 13, 2010; revised January 19, 2011; accepted February 6, 2011